AMERICAN SOCIETY FOR MICROBIOLOGY | mBio®

RESEARCH ARTICLE

Global Transcriptional Repression of Diguanylate Cyclases by MucR1 Is Essential for *Sinorhizobium*-Soybean Symbiosis

Meng-Lin Li,[a] Jian Jiao,[a] Biliang Zhang,[a] Wen-Tao Shi,[a] Wen-Hao Yu,[a] Chang-Fu Tian[a]

[a]State Key Laboratory of Agrobiotechnology, MOA Key Laboratory of Soil Microbiology, and Rhizobium Research Center, College of Biological Sciences, China Agricultural University, Beijing, China

ABSTRACT The ubiquitous bacterial second messenger c-di-GMP is intensively studied in pathogens but less so in mutualistic bacteria. Here, we report a genome-wide investigation of functional diguanylate cyclases (DGCs) synthesizing c-di-GMP from two molecules of GTP in *Sinorhizobium fredii* CCBAU45436, a facultative microsymbiont fixing nitrogen in nodules of diverse legumes, including soybean. Among 25 proteins harboring a putative GGDEF domain catalyzing the biosynthesis of c-di-GMP, eight functional DGCs were identified by heterogenous expression in *Escherichia coli* in a Congo red binding assay. This screening result was further verified by *in vitro* enzymatic assay with purified full proteins or the GGDEF domains from representative functional and nonfunctional DGCs. In the same *in vitro* assay, a functional EAL domain catalyzing the degradation of c-di-GMP into pGpG was identified in a protein that has an inactive GGDEF domain but with an active phosphodiesterase (PDE) function. The identified functional DGCs generally exhibited low transcription levels in soybean nodules compared to free-living cultures, as revealed in transcriptomes. An engineered upregulation of a functional DGC in nodules led to a significant increase of c-di-GMP level and symbiotic defects, which were not observed when a functional EAL domain was upregulated at the same level. Further transcriptional analysis and gel shift assay demonstrated that these functional DGCs were all transcriptionally repressed in nodules by a global pleiotropic regulator, MucR1, that is essential in *Sinorhizobium*-soybean symbiosis. These findings shed novel insights onto the systematic regulation of c-di-GMP biosynthesis in mutualistic symbiosis.

IMPORTANCE The ubiquitous second messenger c-di-GMP is well-known for its role in biofilm formation and host adaptation of pathogens, whereas it is less investigated in mutualistic symbioses. Here, we reveal a cocktail of eight functional diguanylate cyclases (DGCs) catalyzing the biosynthesis of c-di-GMP in a broad-host-range *Sinorhizobium* that can establish nitrogen-fixing nodules on soybean and many other legumes. These functional DGCs are generally transcribed at low levels in soybean nodules compared to free-living conditions. The engineered nodule-specific upregulation of DGC can elevate the c-di-GMP level and cause symbiotic defects, while the upregulation of a phosphodiesterase that quenches c-di-GMP has no detectable symbiotic defects. Moreover, eight functional DGCs located on two different replicons are all directly repressed in nodules by a global silencer, MucR1, that is essential for *Sinorhizobium*-soybean symbiosis. These findings represent a novel mechanism of a strategic regulation of the c-di-GMP biosynthesis arsenal in prokaryote-eukaryote interactions.

KEYWORDS c-di-GMP, diguanylate cyclase, nodule, rhizobia

Cyclic dimeric GMP (c-di-GMP) is a ubiquitous second messenger in bacteria, regulating key functions and mechanisms such as biofilm formation, transition from motility to sessility, cell cycle, and differentiation (1). Most of these pathways are involved in bacterial interactions with abiotic surfaces or with other bacterial and eukaryotic cells (1, 2). c-di-GMP is a diffusible intracellular molecule synthesized from two

Citation Li M-L, Jiao J, Zhang B, Shi W-T, Yu W-H, Tian C-F. 2021. Global transcriptional repression of diguanylate cyclases by MucR1 is essential for *Sinorhizobium*-soybean symbiosis. mBio 12: e01192-21. https://doi.org/10.1128/mBio.01192-21.

Editor Anne K. Vidaver, University of Nebraska-Lincoln

Address correspondence to Chang-Fu Tian, cftian@cau.edu.cn.

Received 22 April 2021
Accepted 22 September 2021
Published 26 October 2021

GTP molecules by diguanylate cyclases (DGCs) containing the GGDEF domain and can be degraded into 5′-phosphoguanylyl-(3′–5′)-guanosine (pGpG) and/or two GMP molecules by phosphodiesterases (PDEs) bearing the EAL or HD-GYP domains (3, 4). c-di-GMP homeostasis is modulated by DGCs and PDEs and can be sensed by effectors, including the PilZ domain, GIL domain, MshEN domain, riboswitch, transcriptional factors, and degenerate GGDEF or EAL domain (4, 5). The high diversity in DGCs, PDEs, and c-di-GMP effectors and their subsequent regulation accounts for the multiple roles of c-di-GMP in bacterial adaptations to fluctuating abiotic and biotic conditions.

c-di-GMP signaling has been mainly and intensively studied in bacterial pathogens but less so in mutualistic bacteria (2, 6–12). As model mutualistic microsymbionts, rhizobia induce and intracellularly infect root nodules, where they fix atmospheric N_2 into ammonia to support legume growth (13). The energy-consuming process of rhizobial nitrogen fixation is sustained by nutrients provided by host cells (14). Rhizobia can live saprophytically in soils in the absence of a compatible legume host and represent a typical facultative microsymbiont bearing larger genomes than those obligate microsymbionts to cope with fluctuating stimuli (15). Constitutive expression of a DGC (PleD) from *Caulobacter crescentus* in *Rhizobium etli* and *Rhizobium leguminosarum* strains favored exopolysaccharide (EPS) production and adhesion to legume roots but decreased the fresh weight of inoculated plants (9). A similar constitutive expression of PleD from *C. crescentus* in *Sinorhizobium meliloti* allowed the discovery of cryptic EPSs such as a linear mixed-linkage beta-glucan and an arabinose-containing polysaccharide (6, 7, 12), although the plasmid carrying this heterologous PleD was lost rapidly under nonselective conditions, including the rhizosphere of the legume host alfalfa (7). A later study showed that an *S. meliloti* mutant lacking 16 out of 17 GGDEF-encoding genes had no salient phenotypes under tested free-living and symbiotic conditions except for its decreased tolerance to acid stress (11), although this strain had no detectable c-di-GMP under test conditions. In contrast, a c-di-GMP-free derivative of *C. crescentus* showed severe defects in its bimodal life cycle, motility, and surface attachment (16), and a *Salmonella enterica* serovar Typhimurium mutant lacking all GGDEF-encoding genes lost virulence and exhibited various defects in free-living processes, such as motility, biofilm formation, and cellulose biosynthesis (17). In short, despite open pangenomes of rhizobial species and dozens of c-di-GMP signaling components in individual genomes (10, 18), c-di-GMP signaling in rhizobia remains largely unexplored.

In this work, we focused on *Sinorhizobium fredii* CCBAU45436 (SF45436), which can establish effective symbiosis with soybean and many other legumes (19, 20). A genome-wide bioinformatic analysis of proteins with putative GGDEF, EAL, and HD-GYP domains was performed. The functional DGCs were screened by heterogenous expression of the full proteins or GGDEF domain alone in *Escherichia coli* in a canonical Congo red binding assay. Enzymatic activities of DGC or PDE were further tested for purified full proteins, GGDEF or EAL domains from representative functional, and nonfunctional DGCs. Transcriptome sequencing (RNA-seq) was used to determine transcriptional profiles of DGCs at exponential and stationary phases in free-living culture and in soybean nodules. The potential role of c-di-GMP in symbiosis was tested by using deletion mutants of major DGCs transcribed in soybean nodules or engineered strains harboring nodule-specific overexpression of a functional DGC or an active EAL domain. Finally, we studied the direct transcriptional regulation of functional DGCs by a pleotropic regulator, MucR, which modulates various canonical processes responding to c-di-GMP (21) and is essential for symbiotic efficiency of SF45436 on soybean (22).

RESULTS AND DISCUSSION

Screening functional diguanylate cyclases in *Sinorhizobium fredii* SF45436. Genome-wide analysis of *S. fredii* SF45436 uncovered 25 GGDEF-containing proteins, which show various domain organizations (Fig. 1A). Putative receptors of c-di-GMP and phosphodiesterases (PDE) were also identified, indicating that complete c-di-GMP signaling may exist in SF45436. Similar numbers of c-di-GMP signaling components are in complete genomes of other *Sinorhizobium* strains associated with soybeans (23, 24),

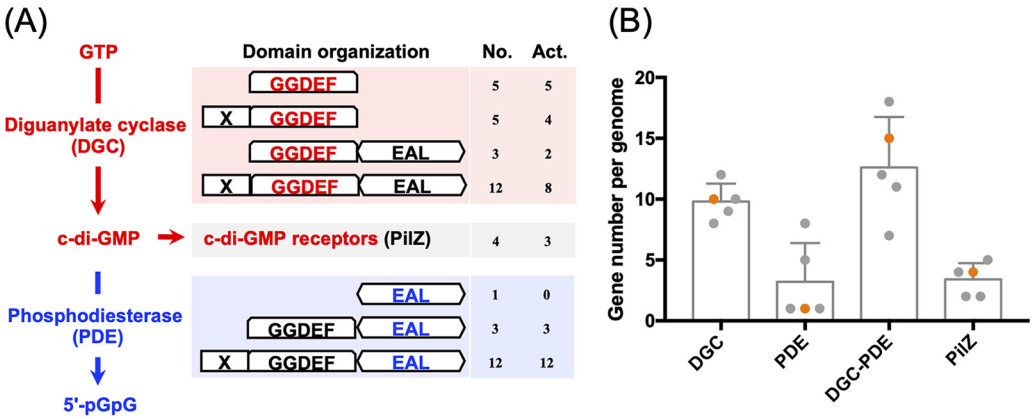

FIG 1 Overview of c-di-GMP signaling in *Sinorhizobium fredii* SF45436. (A) Synthesis of c-di-GMP by diguanylate cyclase (DGC) harboring the GGDEF domain and degradation of c-di-GMP by phosphodiesterase (PDE) containing the EAL domain. X indicates various sensory domains. The number of proteins, with each corresponding domain organization form, encoded by the SF45436 genome is shown (No.). Among them, the number of proteins with a conserved active motif [$D_{X(7\ aa)}N_{X(8\ aa)}D_{X(21\ aa)}R_XG_{/S/A}GD_{/E}EF$] is indicated (Act). (B) The number of genes encoding proteins with putative activity of DGC or PDE, DGC-PDE bifunctional proteins, or PilZ-like proteins in *Sinorhizobium* sibling species. The point in orange corresponds to the value of SF45436. The other test *Sinorhizobium* strains include *S. fredii* SF25509, *S. fredii* SF83666, *S. sojae* SJ05684, and *Sinorhizobium* sp. strain SS05631. Error bars represent SD.

such as *S. fredii* SF25509 (26 proteins), *S. fredii* SF83666 (35 proteins), *S. sojae* SJ05684 (26 proteins), and *Sinorhizobium* sp. strain SS05631 (28 proteins) (Fig. 1B).

Among those GGDEF-containing proteins in SF45436 (Fig. 2A), 19 of them have GGDEF domains of a conserved motif [$D_{X(7\ aa)}N_{X(8\ aa)}D_{X(21\ aa)}R_XG_{/S/A}GD_{/E}EF$] reported in functional diguanylate cyclases (1). In *E. coli*, the c-di-GMP biosynthesis mediated by a functional diguanylate cyclase can be indicated by the biosynthesis of cellulose with strong Congo red binding ability (25). To verify the activity of putative diguanylate cyclases in SF45436, Congo red binding ability of *E. coli* strains expressing individual GGDEF-containing proteins from SF45436 was tested (Fig. 2B). Western blot analysis showed notable induced expression by isopropyl-β-D-thiogalactopyranoside (IPTG) for individual proteins in *E. coli* BL21 or Rosetta, although leak expression was observed for those strains harboring *ydeH*, *SFb59510*, *SFc17580*, and *SFc05240* (Fig. 2B). Similar to the known diguanylate cyclase YdeH from *E. coli* (26), overexpressing SFc17580, SFc15850, SFc19200, SFc31640, SFb52570, SFc11920, SFc23720, and SFb47640 from SF45436 was able to enhance the ability of engineered *E. coli* cells to bind Congo red. All eight of these proteins and YdeH have the conserved motif [$D_{X(7\ aa)}N_{X(8\ aa)}D_{X(21\ aa)}R_XG_{/S/A}GD_{/E}EF$], while overexpression of some other proteins with this motif could not enable *E. coli* to bind Congo red (Fig. 2B).

Diverse N-terminal domains, such as REC-REC (SFc19200), 5TM-5TMR_LYT-PAS_4-PAS_7 (SFc31640), CHASE4 (SFc11920), and HAMP-PAS (SFb47640 and SFc23720), are associated with GGDEF in these functional DGCs, implying their potential roles in directly sensing fluctuating stimuli or interacting with other proteins in the life cycle of this facultative microsymbiont of various legumes (19, 20, 27). For example, diverse PAS domains can serve as direct sensors of various ligands, including oxygen, blue light, cellular redox, carboxylate-containing substrates, divalent metal, and fatty acid (28). DGCs with the REC domain are responsive regulators of two-component signal transduction systems, responding to extracellular or intracellular signals perceived by their cognate sensor His kinases (1). When only the GGDEF domain from 20 proteins of multiple domains was overexpressed in *E. coli*, none of them was functional (see Fig. S1 in the supplemental material). Since stable single GGDEF-domain-bearing DGCs are not rare (Fig. 2B), this implies potential misfolding of the cloned GGDEF domain from SFc19200, SFc31640, SFb52570, SFc11920, SFc23720, and SFb47640. This view was further supported by high-performance liquid chromatography mass spectrometry (HPLC-MS) analysis of c-di-GMP production using purified His-

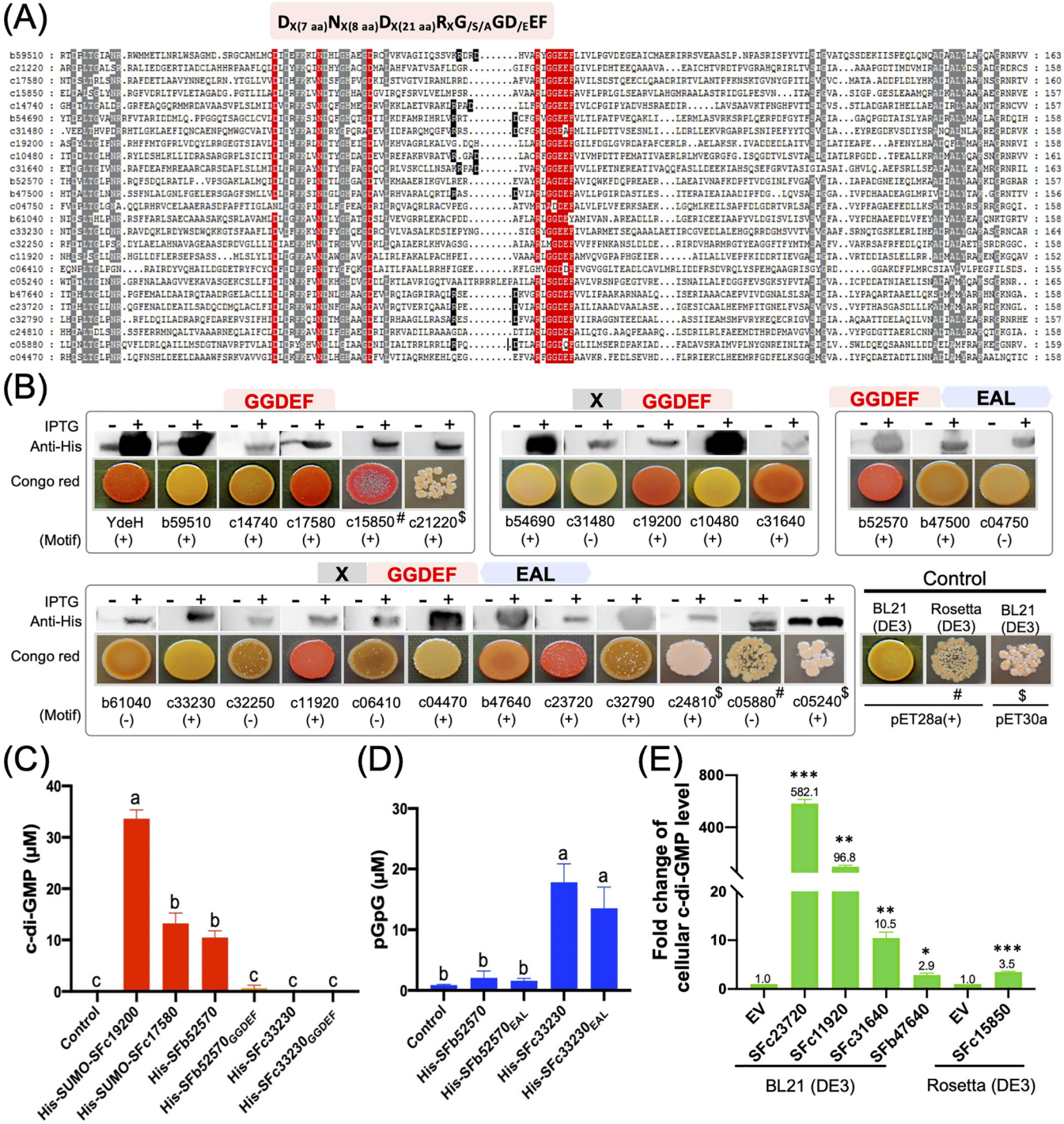

FIG 2 Characterization of the GGDEF-containing proteins from *S. fredii* SF45436. (A) A sequence alignment of the GGDEF domain. A reported conserved motif essential for functional DGCs is shown. Gray background indicates other conserved amino acids in this sequence alignment (present in more than 80% sequences). Residues in black background form the reported allosteric I site involved in product inhibition of c-di-GMP synthesis. (B) Congo red binding ability of *E. coli* strains harboring various GGDEF-containing proteins from SF45436. Western blotting with anti-His monoclonal antibody shows the induced expression of corresponding proteins by IPTG. (+) and (−) indicate proteins with/without a conserved active motif [$D_{X(7\ aa)}N_{X(8\ aa)}D_{X(21\ aa)}R_XG_{/S/A}GD_{/E}EF$]. YdeH is a known functional DGC from *E. coli*. For proteins not expressed in BL21(DE3) harboring pET28a(+) derivatives, the Rosetta strains (#) containing the same expressing plasmids or BL21(DE3) carrying pET30a derivatives ($) were tested. (C and D) HPLC-MS determination of c-di-GMP (C) or pGpG (D) content in 1 μM purified protein prepared from *E. coli* strains harboring corresponding vectors derived from pET30a or pET28a(+). Error bars represent standard deviations. Different letters above error bars indicate significant difference between means based on three independent experiments (ANOVA followed by Bonferroni's multiple-comparison test, $\alpha = 0.05$). (E) HPLC-MS determination of c-di-GMP content in *E. coli* strains expressing the indicated proteins relative to that of strains carrying the empty vector (*, $P < 0.05$; **, $P < 0.01$; ***, $P < 0.001$; *t* test). Error bars represent SD. Protein purification for these five proteins was not successful under test conditions, and *in vitro* enzymatic assay was not done.

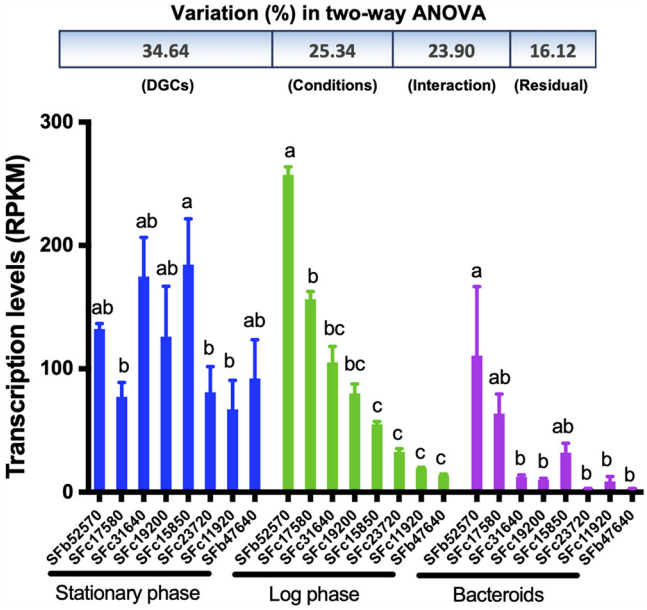

FIG 3 Transcription profiles of functional diguanylate cyclases in free-living and symbiotic SF45436. Different letters indicate significant differences between means of three biological replicates (two-way ANOVA followed by Bonferroni's multiple-comparison test under each condition; $\alpha = 0.05$). RPKM, reads per kilobase per million mapped reads. Error bars represent SEM.

SFb52570$_{GGDEF}$ and His-SFb52570 (Fig. S2) in the presence of GTP, i.e., the full protein of SFb52570 rather than SFb52570$_{GGDEF}$ alone had diguanylate cyclase activity (Fig. 2C). Moreover, phosphodiesterase activity was not detectable for His-SFb52570$_{EAL}$ and His-SFb52570, suggesting a degenerated EAL domain in this protein (Fig. 2D). The degenerate EAL domain of SFb52570 may play a structural or regulatory function, as deletion of this enzymatically inactive EAL domain abolished the DGC activity of SFb52570 (Fig. 2C, Fig. S1). Similarly, DGCs with degenerate EAL domains are also experimentally demonstrated in *Gluconacetobacter xylinus* (29, 30).

Both purified His-SFc33230 and His-SFc33230$_{EAL}$ (Fig. S2) exhibited phosphodiesterase activity generating 5′-pGpG from c-di-GMP, whereas no diguanylate cyclase activity was detected for His-SFc33230 and His-SFc33230$_{GGDEF}$ (Fig. 2D and C). The purified His-SUMO-SFc17580 with only the GGDEF domain and His-SUMO-SFc19200 (Fig. S2; His-SFc17580 and His-SFc19200 were poorly soluble) were able to produce c-di-GMP from GTP (Fig. 2C). Although protein purification for the other five functional DGCs (SFc23720, SFc11920, SFc31640, SFb47640, and SFc15850) was not successful under test conditions, HPLC-MS analysis revealed significantly higher levels of c-di-GMP in *E. coli* strains expressing these five DGCs than in strains carrying empty vectors (Fig. 2E; $P < 0.05$, *t* test). These results are consistent with those of Congo red binding assay.

Transcriptional profiles of functional diguanylate cyclases and the effect of c-di-GMP elevation in soybean nodules. RNA-seq analysis revealed that eight functional diguanylate cyclases exhibited contrasting transcriptional profiles during exponential (log) and stationary phases and within soybean nodules (Fig. 3). The largest proportion of total variation (34.64%) was explained by different diguanylate cyclases, followed by different conditions (25.34%) and interaction between these two main effects (23.9%). SFb52570 and SFc17580 were major diguanylate cyclases transcribed during the log phase and within symbiotic nodules (Fig. 3), although all functional DGCs were actively transcribed at stationary phase, suggesting that multiple stress signals arise under this nutrient-starving condition. In line with these findings, two DGCs had relatively strong expression during all growth phases of *E. coli*, while a number of DGCs were induced during stationary phase (25).

In-frame deletion of either *SFb52570* (Δ*b52570*) or *SFc17580* (Δ*c17580*) or both major DGC genes (Δ*c17580* Δ*b52570*) had no significant symbiotic defects on soybean

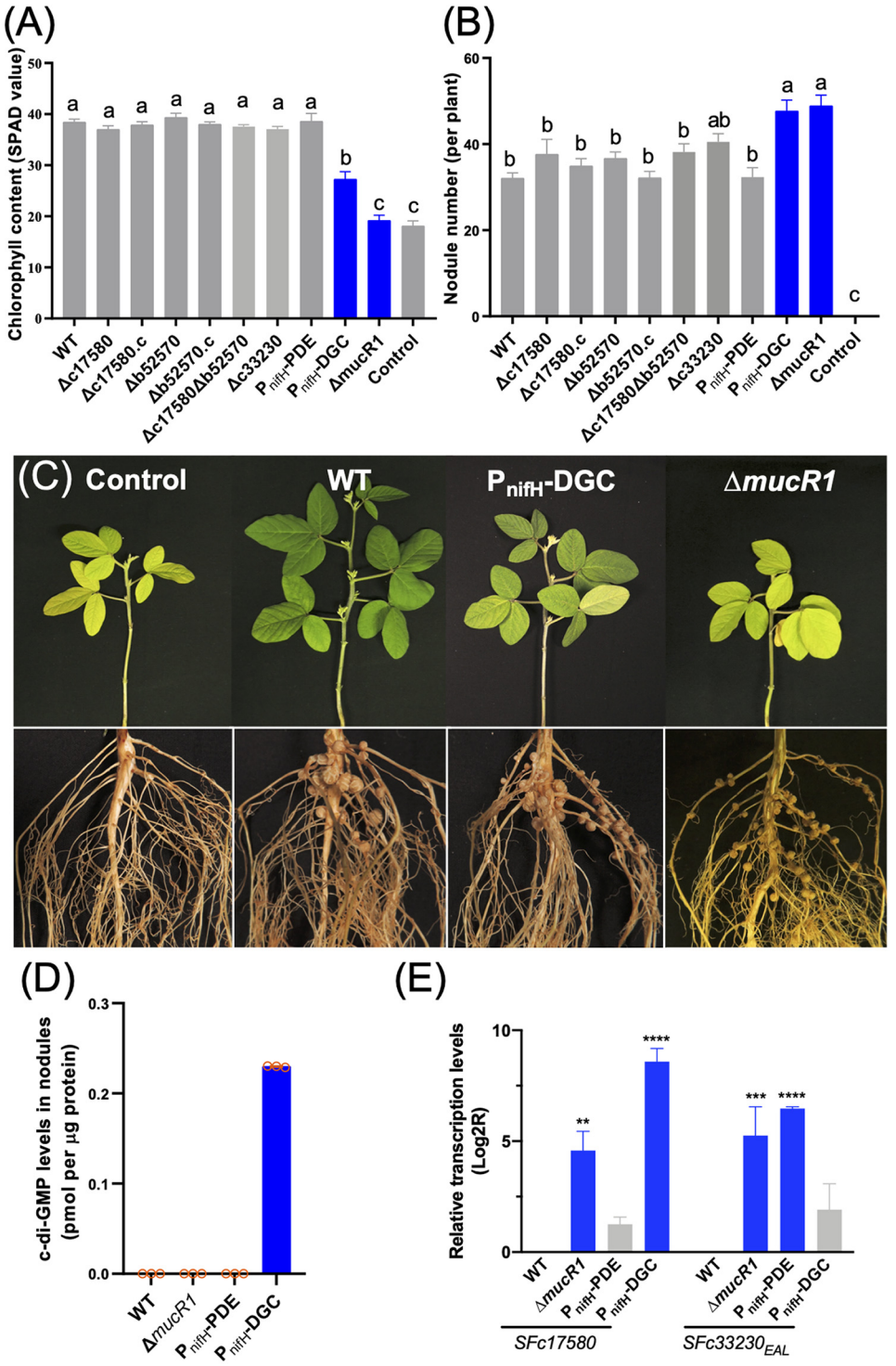

FIG 4 Symbiotic defects mediated by c-di-GMP overload in soybean nodules. (A) Chlorophyll content. (B) Nodule number per plant. Test strains include deletion (Δ) or complementary (.c) strains for DGC genes (*SFc17580* and *SFb52570*), the deletion mutant of PDE gene (*SFc33230*), and derivatives carrying PDE ($SFc33230_{EAL}$) and DGC (*SFc17580*) driven by the *nifH* (*SFa46030*) promoter P_{nifH}. The Δ*mucR1* mutant was used for comparison. Error bars represent SEM. Different letters indicate significant differences between means based on more than 12 plants (ANOVA followed by Turkey's multiple-comparison test; $\alpha = 0.05$). (C) Pictures indicating yellow leaves and the increased nodule number of soybean plants inoculated with the P_{nifH}-DGC and the Δ*mucR1* mutant. (D) c-di-GMP levels in nodules (three biological replicates; error bars represent SD). (E) Transcriptional changes of *SFc17580* and $SFc33230_{EAL}$ in test strains (three biological replicates, ANOVA followed by Dunnett's multiple comparisons; ***, $P < 0.001$; ****, $P < 0.0001$; error bars represent SD).

plants (Fig. 4A and B). In contrast, a derivative carrying the functional DGC SFc17580 (Fig. 2C) driven by the *nifH* promoter (P_{nifH}-DGC) induced more but inefficient nodules, leading to a significant decline in chlorophyll content of soybean leaves (Fig. 4A to C). Since *nifH* encodes the nitrogenase reductase and is specifically expressed in nodules induced by most rhizobia without free-living nitrogen fixation ability (22, 31), the impaired symbiotic performance of the P_{nifH}-DGC strain is strictly nodule specific. This is in contrast to earlier studies of *R. etli* and *R. leguminosarum* using a constitutive expression version of heterogenous PleD from *C. crescentus*, which showed a decline in both nodule number and nitrogen content of corresponding host plants *Phaseolus vulgaris* and *Vicia sativa* (9). When the transcription of the functional EAL domain of SFc33230 (Fig. 2D) was driven by P_{nifH} (P_{nifH}-PDE), no symbiotic defects were observed on soybean plants (Fig. 4A and B). This is consistent with the normal phenotype of alfalfa plants inoculated with an *S. meliloti* mutant lacking 16 out of 17 GGDEF-encoding genes and having no detectable c-di-GMP (11).

The HPLC-MS analysis (Fig. 4D) further showed that c-di-GMP was at the level of pmol per microgram protein in nodules infected by the PnifH-DGC strain but undetectable in the other treatments (the wild-type SF45436, Δ*mucR1*, and P_{nifH}-PDE strains). Further quantitative reverse transcription-PCR (qRT-PCR) analysis (Fig. 4E) revealed that the DGC gene *SFc17580* and the EAL-encoding fragment $SFc33230_{EAL}$ were actively transcribed in the P_{nifH}-DGC and P_{nifH}-PDE strains, respectively. This demonstrated the efficiency of the test P_{nifH} promoter in nodules, and the high expression of $SFc33230_{EAL}$ had no significant effect on symbiosis. In short, elevating rhizobial c-di-GMP in nodules exerted a negative effect on symbiotic performance.

For comparison, the in-frame deletion mutant of the functional PDE gene *SFc33230* (Fig. 2D) or the pleotropic regulator gene *mucR1* (*mucR2*, the other *mucR* copy in SF45436, is not functional due to a frameshift mutation) (21, 22) were also tested for their symbiotic performance. As many as 31 EAL domain-containing proteins are present in SF45436 (Fig. 1A); consequently, it is not unexpected that Δ*c33230* strain was indistinguishable from the wild-type SF45436 in symbiotic performance (Fig. 4A and B). The Δ*mucR1* mutant showed more severe symbiotic defects than the P_{nifH}-DGC strain regarding the chlorophyll content of leaves (Fig. 4A and C), although it induced as many nodules as the P_{nifH}-DGC strain (Fig. 4B and C). Both *SFc17580* and $SFc33230_{EAL}$ were upregulated in the Δ*mucR1* mutant (Fig. 4E). This may at least partially explain the undetectable c-di-GMP in nodules infected by the Δ*mucR1* mutant, implying an intriguing regulation role of MucR1 on c-di-GMP signaling components.

Moreover, bacteroids of the P_{nifH}-DGC strain and the Δ*mucR1* mutant but not those of the P_{nifH}-PDE strain showed significant upregulation of genes involved in various c-di-GMP-responsive processes (Fig. 5), such as the c-di-GMP receptor McrA, regulating motility (11), and CuxR, activating arabinose-containing polysaccharide production (6), the biosynthesis of mixed-linkage beta-glucan (*bgsA*) and adhesion polysaccharides (*uppE*), and a key flagellar component (*fliG*) (12, 32, 33). Notably, both polysaccharides and motility machinery have energetic cost in bacterial physiology and are downregulated during nitrogen fixation that consumes as many as 16 ATP to reduce one molecule of N_2 (22, 27, 34). This is supported by recent evidence that optimum energy metabolism status of bacteroids is required for efficient symbiosis in soybean nodules (24).

Since no c-di-GMP could be detected in bacteroids of the Δ*mucR1* mutant while the P_{nifH}-DGC strain significantly accumulated c-di-GMP in nodules (Fig. 4E), the transcription of the c-di-GMP-responsive processes mentioned above may be subject to a general negative regulation by MucR1, which can be relieved to a certain extent by elevating c-di-GMP levels (Fig. 5). Notably, MucR1 can also act as a positive regulator required for active transcription of high-affinity transporters for phosphate and zinc ions and the iron-responsive regulator RirA, which are all essential for efficient symbiosis of *S. fredii* within soybean nodules (22, 35–38). The downregulation of *rirA* in bacteroids of the *mucR1* mutant was confirmed in this work but not observed in bacteroids

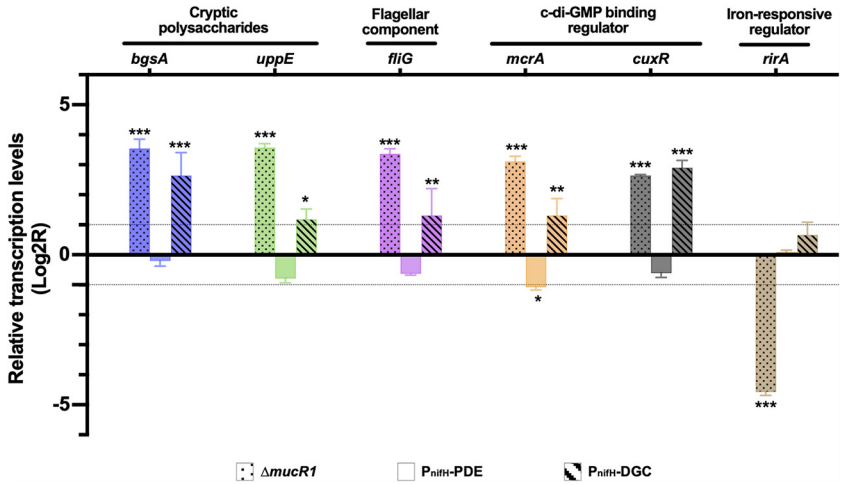

FIG 5 Transcriptional changes of c-di-GMP responsive genes of the Δ*mucR* mutant and the P_{nifH}-DGC and P_{nifH}-PDE strains in soybean nodules. An iron-responsive regulator gene, *rirA*, is used as a control. Significant differences compared to the wild-type SF45436 are indicated (three biological replicates, ANOVA followed by Dunnett's multiple comparisons; **, $P < 0.01$; ***, $P < 0.001$).

of the P_{nifH}-DGC strain (Fig. 5). This may partially explain the more severe symbiotic defects associated with the **Δ***mucR1* mutant than the P_{nifH}-DGC strain (Fig. 4A to C).

Direct regulation of functional DGCs by MucR1. The previous transcriptomic analyses in alphaproteobacteria have revealed various processes responding to c-di-GMP, and some GGDEF/EAL-encoding genes are differentially transcribed when *mucR1* is mutated (21, 22). As mentioned above, certain functional DGCs were transcribed at relatively low levels in bacteroids and exponential-phase cells, although a global active transcription of functional DGCs was observed at the stationary phase (reads per kilobase per million mapped reads [RPKM] > 67; Fig. 3). In line with these transcriptional profiles of functional DGCs, the average RPKM value of *mucR1* in stationary-phase cells was 12% and 52% of those in exponential-phase cells and bacteroids, respectively (Data Set S1). However, the relatively low transcription level of *mucR1* at the stationary phase can still be considered active transcription within the whole transcriptome (RPKM > 156; Data Set S1). qRT-PCR analyses of soybean nodules and the free-living cells in rich medium TY (optical density at 600 nm [OD_{600}] of 1.2) showed that transcriptional levels of most functional DGCs were significantly upregulated in the **Δ***mucR1* mutant compared to the wild-type SF45436 (Fig. 6A and B), with more drastic changes in nodules. The transcription of functional PDE SFc33230 was also significantly upregulated in the **Δ***mucR1* mutant under both symbiotic and free-living conditions (Fig. 6A and B). Although these DGC/PDE genes have a scattered distribution pattern on the chromosome and chromid, the observed overall upregulation transcription profiles, particularly in nodules, imply that these genes are regulated by a shared regulation machinery.

Cumulative evidence suggests the zinc-finger bearing MucR can be a global repressor preferring low-GC target sequences of low consensus (21, 39, 40). Sequence analysis revealed that the average %GC of upstream intergenic region for genes encoding functional or nonfunctional DGCs (Fig. 6C) is significantly lower than the genome average of 63.1% (*, $P < 0.05$; **, $P < 0.01$; *t* test) and the average value of the chromosome (63.45%, $P < 0.05$; *t* test) and chromid (63.04%, $P < 0.05$; *t* test) while indistinguishable from the average %GC of the symbiosis plasmid pSymA (59.92%, $P > 0.097$; *t* test). Further electrophoretic mobility shift assay (EMSA) with the purified Sumo-MucR1 and its derivative MucR1 (with Sumo removed by HRV-3C protease) demonstrated that MucR1 can directly bind the promoter regions of genes encoding eight functional DGCs and the functional PDE SFc33230 (Fig. 6D) but not on three tested

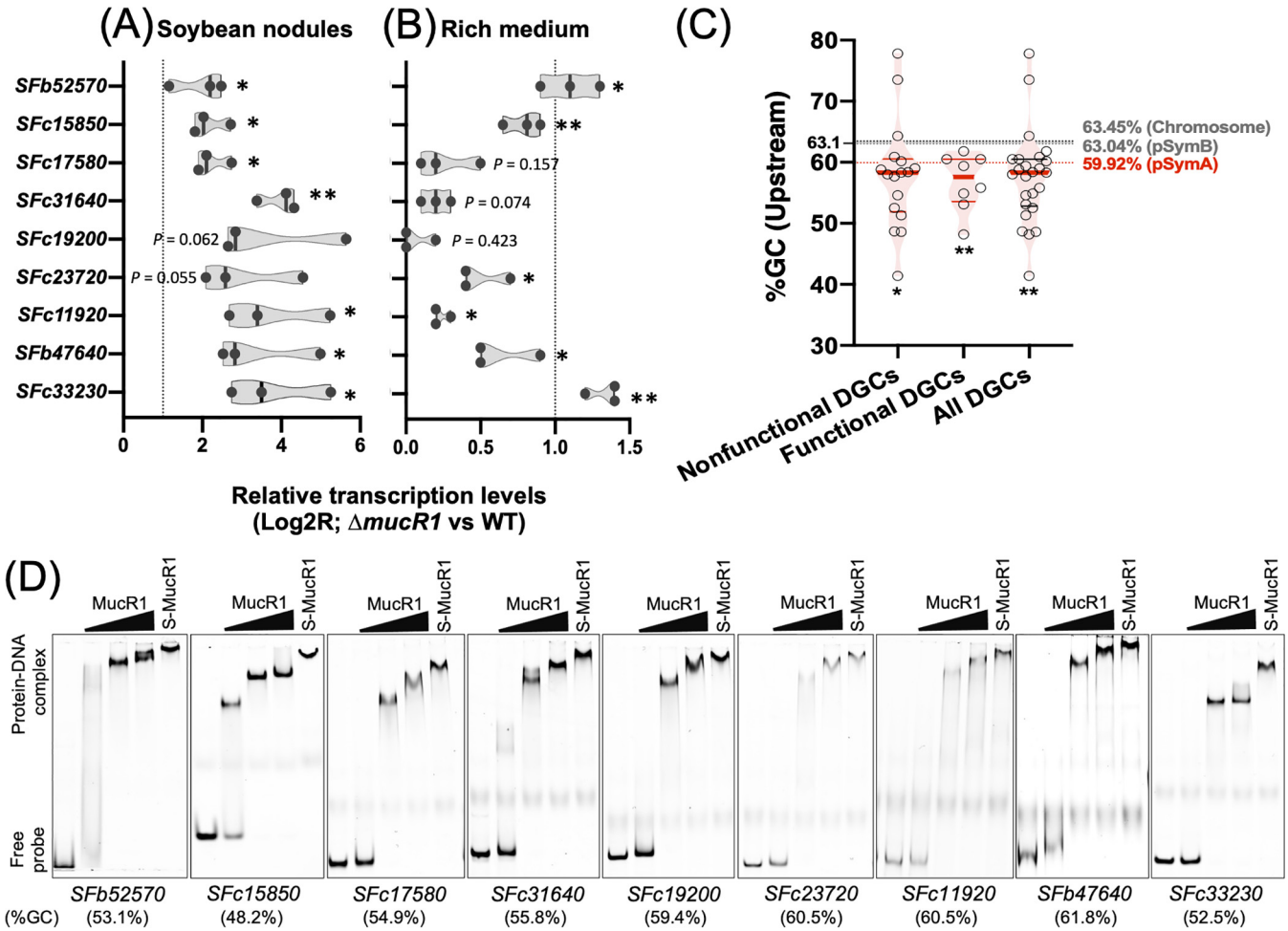

FIG 6 Direct transcriptional repression of eight functional DGCs and the PDE SFc33230 by MucR1 in soybean nodules. (A and B) Transcriptional changes of functional DGC genes in the Δ*mucR1* mutant compared to the wild-type SF45436 in soybean nodules (A) and the TY medium at an OD_{600} of 1.2 (B), based on qRT-PCR (three biological replicates; *, $P < 0.05$; **, $P < 0.01$; *t* test). (C) Average %GC of upstream intergenic region for genes encoding functional or nonfunctional DGCs. The genome average of 63.1% and those average values of three major replicons are shown. Significant difference compared to the genome average value is indicated (*, $P < 0.05$; **, $P < 0.01$; *t* test). (D) MucR1 binds the promoters of genes encoding eight functional DGCs and the PDE SFc33230 in the electrophoretic mobility shift assay (EMSA). The purified Sumo-MucR1 (27 μM, S-MucR1) and its derivative, MucR1 (Sumo was removed by HRV-3C protease), with increasing concentrations (4.5, 13.5, and 27 μM) were incubated with Cy5-labeled DNA probes. %GC of test probes are shown.

nonfunctional DGCs (Fig. S3). A clear gradient of band shift for test probes was observed when the ratio of MucR1 to probe was increased (Fig. 6D), suggesting oligomeric or multiple MucR1 binding events. This is in line with the hypothesis that MucR1 works in a similar nonspecific way in binding DNA as the well-known H-NS (histone-like nucleoid structuring protein) of *E. coli* (21, 40–43). The global repression of functional DGC genes located on different replicons by MucR1, particularly in nodules, represents a largely unexplored scenario in the evolution of the facultative life cycle of rhizobia.

The MucR/Ros family proteins are mainly found in alpha and *deltaproteobacteria*, particularly conserved in the former class that is enriched with various pathogenic and mutualistic bacteria associated with eukaryote hosts (21). Intensive studies of MucR/Ros homologs from *Agrobacterium*, *Sinorhizobium*, *Rhizobium*, *Mesorhizobium*, *Caulobacter*, and *Brucella* uncovered not only the conserved phenotype of rough colonies of the *mucR* or *ros* mutant but also their pleotropic transcriptional regulatory role in various cellular processes, such as the production of exopolysaccharides, motility and chemotaxis, cell cycle, ion uptake, and protein secretion systems (22, 38, 39, 44–53), some of which are involved in symbiosis and virulence. In the model rhizobium *S. meliloti*, for example, MucR directly activates the

transcription of *exoY*, encoding a galactosyltransferase initiating the repeating unit assembly process during the biosynthesis of succinoglycan exopolysaccharide (54) that is essential for *S. meliloti* host invasion (48, 55). MucR can directly repress the transcription of Rem, which is a transcriptional activator of motility genes (56). It has been established that c-di-GMP is a ubiquitous second messenger modulating motility, biofilm formation, virulence, and cell cycle in bacteria (57), and several common cellular process regulated by both c-di-GMP and MucR recently have been reviewed for the free-living lifestyle of *S. meliloti* (58). This work further demonstrated that, at the nitrogen-fixing stage of mutualistic interaction between rhizobium and legumes, MucR can globally repress functional DGCs to downshift various energetically expensive processes induced by c-di-GMP. This strategic regulation mechanism also can be tested in other bacterium-host interactions.

Conclusions. Rhizobia are characterized by their facultative symbiotic life cycle, in which various stimuli should be sensed and properly responded to. Dozens of c-di-GMP signaling components are present in rhizobia but are largely unexplored. This work made a systematic screening of functional DGCs in *S. fredii* SF45436 by using both *in vitro* and *in vivo* experiments (Fig. 1 and 2). The condition-dependent transcriptomic profiles suggest a general downregulation of functional DGC genes in soybean nodules (Fig. 3). An engineered nodule-specific accumulation of c-di-GMP led to an increased number of inefficient nodules, while no c-di-GMP could be detected in efficient nodules infected by the wild-type SF45436 and the PDE-overexpressing strain (Fig. 4). The elevated c-di-GMP induced various c-di-GMP-responsive processes, which are energetically costly and negatively regulated by the pleotropic regulator MucR1 in nodules (Fig. 5). It was further revealed that functional DGCs with scattered distributions in the multipartite genome of SF45436 were all directly repressed by MucR1 through oligomeric or multiple binding events on their promoter regions (Fig. 6). Collectively, these findings demonstrate a strategic repression of the c-di-GMP biosynthesis arsenal in legume nodules (Fig. 7), which represents a novel adaptation mechanism potentially explored by many other prokaryotes harboring a rich pool of c-di-GMP signaling components and their distinct global silencers, such as MucR (alphaproteobacteria, G-), H-NS and MvaT (gammaproteobacteria, G-), Lsr2 (actinobacteria, G^+), and Rok (bacilli, G^+) (21).

MATERIALS AND METHODS

Bacteria and culture conditions. Bacterial strains and plasmids used in this work are shown in Table S1 in the supplemental material. *E. coli* was grown at 37°C in Luria broth (LB) medium. *S. fredii* SF45436 and its derivatives were grown at 28°C in TY medium (tryptone at 5 g/liter, yeast extract at 3 g/liter, and $CaCl_2$ at 0.6 g/liter). The antibiotic concentrations used were 50 μg/ml kanamycin (Km), 10 μg/ml trimethoprim (Tmp), 30 μg/ml gentamicin (Gen), and 30 μg/ml carbenicillin (Cb).

Genetic procedures. The primers used are listed in Table S2. All plasmid constructs in this work were verified by Sanger sequencing. Plasmids were transformed into *E. coli* DH5α (unless indicated) before conjugation into rhizobia with pRK2013 as the helper plasmid.

The Δ*mucR1* mutant was generated by removing the gentamicin resistance cassette within the Δ*mucR1*::*Gm* mutant constructed previously (22). The pCM157 plasmid carrying Cre recombinase that recognizes the *loxP* sites flanking the gentamicin cassette was introduced into the Δ*mucR1*::*Gm* mutant, and transconjugants sensitive to gentamicin were selected for subsequent screening of pCM157-cured strains (59). To construct in-frame deletion mutations of *SFc33230*, *SFc17580*, and *SFb52570*, a seamless assembly method was used. Briefly, gene-flanking regions of 500 to 1,000 bp were amplified using primers carrying 5′-homologous sequences containing the ends of SmaI restriction sites (CCC) in pJQ200SK (60). Two flanking fragments were mixed with SmaI-linearized pJQ200SK and incubated at 50°C for 15 min using a seamless cloning kit (Taihe Biotechnology), and positive transformants with correct sequences were used for conjugation with SF45436. Single-crossover clones resistant to Gen were selected for sequencing verification and subsequent cultivation in liquid TY medium for 36 h. The resulting liquid culture was subjected to double-crossover screening on a TY plate containing 7% (wt/vol) sucrose and Tmp as previously described (61).

Individual coding sequences for 26 DGCs (including YdeH from *E. coli* K-12), 20 GGDEF domains, and two EAL domains ($SFc33230_{EAL}$ and $SFb52570_{EAL}$) were amplified using primers harboring 5′-homologous sequences, including the ends of the NdeI restriction site (CAT) of pET28a(+), or primers carrying 5′-homologous sequences, including the ends of BamHI site (GGA) of pET30a-SUMO. These amplified fragments were individually subjected to seamless cloning with the plasmids pET28a(+) and pET30a-SUMO linearized by NdeI and BamHI, respectively. The resulting plasmids were then transformed into *E. coli* BL21(DE3) or Rosetta(DE3) before Congo red binding assay or protein purification experiments.

To construct pJQ-P_{nifH}-c17580 and pJQ-P_{nifH}-$c33230_{EAL}$, a promoter region (496 bp of *SF45436_a46030*) and the upstream and downstream fragments of the coding sequences of *SFc17580* or $SFc33230_{EAL}$ were amplified using primers containing the ends of the SmaI restriction site of pJQ200SK. These fragments were linked with pJQ200SK linearized by SmaI using the seamless assembly method described above.

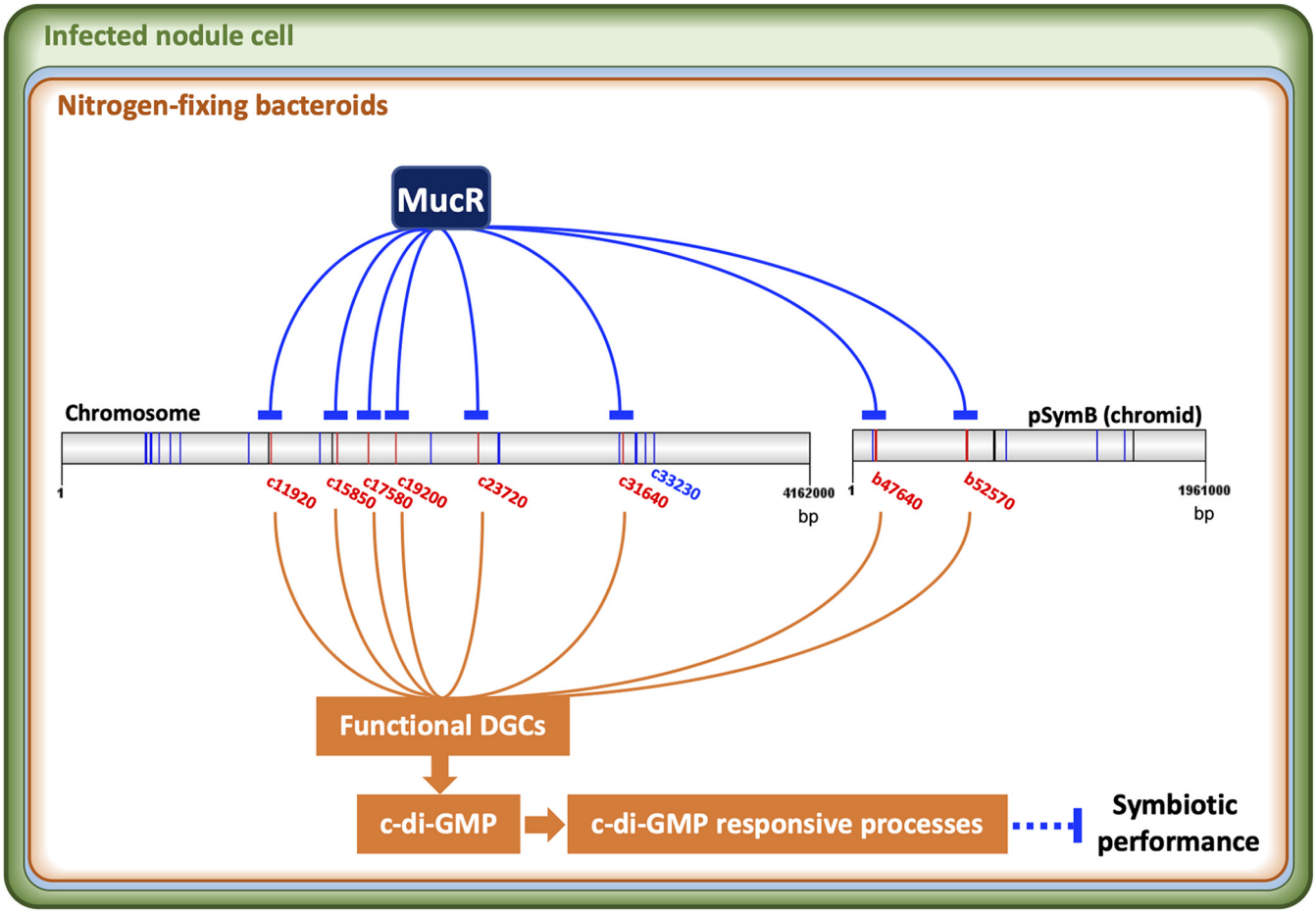

FIG 7 Global repression of functional DGC genes located on chromosome and chromid by MucR in efficient soybean nodules. Genes encoding functional and nonfunctional DGCs are in red and blue, respectively. Artificial accumulation of c-di-GMP in nodules by using PnifH-c17580 leads to upregulation of various c-di-GMP responsive processes and impairs symbiotic performance. Other regulators can be involved in the coordinated regulation of these DGC genes under different conditions but have not been identified yet. Circular replicons (chromosome and chromid) are linearized here for presentation purpose.

The EZ-T Simple Zero pTOPO cloning kit (GenStar) was used to clone intergenic regions, which were then used as DNA probes in EMSA.

Protein expression and purification. *E. coli* BL21(DE3) or Rosetta(DE3) carrying the expression plasmids were grown in LB medium until the OD_{600} had reached 0.8. Gene expression was induced by adding 0.2 mM IPTG for 14 h at 18°C. The cells were harvested (4,000 × *g*, 5 min, 4°C) and resuspended in a lysis buffer (25 mM Tris-HCl, pH 8.0, 250 mM NaCl, 50 mM imidazole, 5% glycerol), supplemented with EDTA-free protease-inhibitor cocktail (1 tablet/50 ml buffer; Roche) and 200 μg/ml lysozyme. After sonication, the supernatant was loaded onto nickel columns washed with the same lysis buffer as described above and eluted with gradient imidazole elution from 100 mM to 500 mM. For the enzyme assay, the elution fractions were purified by size exclusion chromatography using a Superdex 200 10/30 column (GE Healthcare) and the SEC buffer (20 mM Tris-HCl, pH 8.0, 250 mM NaCl, 5% glycerol).

Congo red binding assays. *E. coli* BL21(DE3) or Rosetta(DE3) strains containing pET28a(+) or pET30a-SUMO were grown overnight, subcultured in fresh LB medium, and grown to an OD_{600} of 0.8. Next, 5 μl culture was dropped onto the LB agar medium containing Congo red (50 μg/ml) and IPTG (0.5 mM). Plates were incubated at 23°C, 28°C, and 37°C for 3 days before recording, and the Congo red binding phenotype at 23°C was more obvious under test conditions and was shown in Fig. 2 and Fig. S1.

Western blotting. To determine relative expression levels of cloned genes in *E. coli* strains used in Congo red binding assay, bacteria cultured in LB medium at an OD_{600} of 0.8 were subject to protein expression induced by 0.5 mM (final concentration) IPTG (23°C for 16 h). Cells from pre- and postinduction cultures (adjusted to OD_{600} of 0.8) were harvested by centrifugation (14,000 × *g* for 2 min, 4°C). The pellets were resuspended in SDS-loading buffer and lysed by boiling for 5 min. Each lysate was separated on SDS-PAGE gels and then transferred to nitrocellulose membrane. For immunodetection of individual proteins, HRP (horseradish peroxidase)-conjugated anti-His-Tag mouse monoclonal antibody (CWBIO, China) and ECL Western detection reagents (Solarbio, China) were used.

Enzyme assays. HPLC-MS was used to analyze DGC/PDE activity. The c-di-GMP synthesis assay was measured in a reaction mixture (100 μl) containing 75 mM Tris-HCl (pH 8.0), 250 mM NaCl, 25 mM KCl, 10 mM $MgCl_2 \cdot 6H_2O$, 478 μM GTP (Sigma), and 1 μM protein (26). The c-di-GMP hydrolysis assay was

measured in a reaction mixture (100 μl) consisting of 100 mM Tris-HCl (pH 8.0), 20 mM KCl, 25 mM $MgCl_2 \cdot 6H_2O$, 340 μM c-di-GMP, and 1 μM protein. The mixtures were incubated at 37°C for 12 h and stopped by heating the sample for 5 min at 95°C (29). The supernatants obtained by centrifugation for 10 min at 12,500 $\times$ *g* were filtered through a 0.2-μm syringe filter. Nucleotides were separated and analyzed on a C_{18} reverse-phase column (62).

Plant assays. Symbiotic performance of *S. fredii* strains was tested on *Glycine max* cv. JD17. Seeds were surface sterilized, germinated, and inoculated as previously described (35). At 35 days postinoculation (dpi), leaf chlorophyll content for three leaflets of the third leaf was determined by a SPAD-502 m (Konica Minolta) and nodule numbers were counted. Three independent experiments were performed.

Quantification of c-di-GMP in bacterial cultures and soybean nodules. *E. coli* BL21(DE3) or Rosetta(DE3) cells carrying empty vectors or expression vectors were cultured and subject to IPTG induction as described above for Western blot analysis. Cells were harvested (4,000 $\times$ *g*, 8 min, 4°C) and washed by physiological saline twice. For nodule samples, nodules at 35 dpi were ground with mortar in liquid nitrogen. The resultant bacterial cells or nodule samples were resuspended with extraction solution (acetonitrile-methanol-water at 2:2:1 [vol/vol/vol]) as previously described (63). The resultant 600-μl extraction solution was analyzed by HPLC-MS/MS with c-di-GMP (MedChemExpress, USA) as an internal standard. To determine total protein concentrations of samples, all pellets were resuspended in 800 μl of 0.1 M NaOH and heated at 95°C for 30 min. The soluble samples were centrifuged at 12,000 $\times$ *g* for 5 min and the total protein content was then determined by using bicinchoninic acid (BCA) protein assay kit (ZOMANBIO). Three independent experiments were performed.

RNA-seq analysis. The bacterial cultures of SF45436 carrying pBBRMCS-3 grown in 50 ml TY medium were harvested during log phase (OD_{600}, ~0.5) or stationary phase (OD_{600}, ~4.2). RNA was isolated from bacterial cultures with the bacterial total RNA kit (ZOMANBIO). For bacteroid samples, nodules collected at 35 dpi were subject to RNA extraction using the Qiagen RNeasy minikit. Three biological replicates were performed. Strand-specific RNA sequencing was carried out by Novogene using an Illumina HiSeq platform (Illumina). Clean reads were mapped to the genome of SF45436 using Bowtie2 (default parameters) (23, 64). The number of unique mapped reads for each protein-coding gene was extracted from sorted bam files by HTseq-count (-a 0) (65). Reads per kilobase per million mapped reads (RPKM) were calculated for individual genes and are shown in Data Set S1.

qRT-PCR. SF45436 and its derivatives were grown in 50 ml of TY liquid medium overnight to an OD_{600} of 1.2. The RNA of bacteria was extracted as described above. Isolation of RNA from 35-dpi nodules of *G. max* cv. JD17 was performed using the total RNA kit (Promega). cDNA was synthesized by using the FastKing genomic DNA dispelling RT supermix (TIANGEN). qPCR was performed by using QuantStudioTM 6 Flex and 2$\times$ RealStar green mixture (Genstar). The 16S rRNA gene was used as the reference for normalization of gene expression. Three independent biological replicates were analyzed.

EMSA. The 45-bp Cy5-04750IR probe was generated by annealing the synthesized sense (5′-Cy5) and antisense single-stranded DNA. The other DNA probes were amplified by PCR with the pTOPO plasmid carrying intergenic regions as templates and labeled with Cy5 at 5′ ends, generating Cy5-DNA. The reaction mixture (10 μl) consisted of 0.5 mg/ml bovine serum albumin, 0.1 mg/ml sonicated salmon sperm DNA, 12.3 nM Cy5-DNA, 25 mM Tris-HCl (pH 8.0), 5% glycerol, 0.05% n-dodecyl-β-D-maltoside, and various concentrations of test proteins. The samples were incubated at 20°C for 30 min. Next, 1 μl HRV-3C protease (200 ng/μl; 10 mM dithiothreitol) was mixed well and incubated for a further 30 min. The samples were separated in a 6% TB polyacrylamide gel (no EDTA), and the gel was scanned with a Typhoon FLA 9000 imager (GE Healthcare).

Bioinformatic and statistical analyses. Protein domains were predicted using the NCBI Conserved Domains Database (https://www.ncbi.nlm.nih.gov/Structure/bwrpsb/bwrpsb.cgi). For predicting enzymatic activity of GGDEF, EAL, and PilZ domains, the retrieved protein sequences were aligned with those of proteins with demonstrated enzyme activity. For the GGDEF domain, it was predicted to be active in DGC function if the motif $D_{X(7\ aa)}N_{X(8\ aa)}D_{X(21\ aa)}R_XG_{/S/A}GD_{/E}EF$ was present. Domains containing the RxxD motif located five residues upstream of the GGDEF motif were considered to have an intact allosteric inhibitory site (I-site). For the EAL domain, $E_{X(55\sim58\ aa)}N_{X(31\ aa)}E_{XX}E_{(26\ aa)}D_{(20\ aa)}K_{(35\ aa)}E$ was taken as evidence for putative PDE activity. For predicting c-di-GMP receptors carrying the PilZ domain, the motif $R_{XXX}R_{(20\sim30\ aa)}D/N_XS/A_{xx}G$ was used (1). A domain was considered degenerate if at least one essential residue mentioned above did not match.

GraphPad Prism version 9.0.2 was used to perform statistical analysis, including *t* test and one-way and two-way ANOVA (analysis of variance), followed by multiple-comparison tests as shown in the figure legends ($\alpha = 0.05$).

Data availability. Raw sequence data from our RNA-seq analyses can be accessed via NCBI Sequence Read Archive (PRJNA723738).

SUPPLEMENTAL MATERIAL

Supplemental material is available online only.

DATA SET S1, XLSX file, 1 MB.

FIG S1, PDF file, 0.7 MB.

FIG S2, PDF file, 0.1 MB.

FIG S3, PDF file, 0.1 MB.

TABLE S1, PDF file, 0.2 MB.

TABLE S2, PDF file, 0.2 MB.

ACKNOWLEDGMENTS

This work was supported by the National Key R&D Program of China (grant number 2019YFA0904700), the National Natural Science Foundation of China (32070078), and the Innovative Project of State Key Laboratory of Agrobiotechnology (2020SKLAB1-5). The funders had no role in study design, data collection and interpretation, or the decision to submit the work for publication.

We declare that we have no competing interests.

REFERENCES

1. Römling U, Galperin MY, Gomelsky M. 2013. Cyclic di-GMP: the first 25 years of a universal bacterial second messenger. Microbiol Mol Biol Rev 77:1–52. https://doi.org/10.1128/MMBR.00043-12.
2. Valentini M, Filloux A. 2019. Multiple roles of c-di-GMP signaling in bacterial pathogenesis. Annu Rev Microbiol 73:387–406. https://doi.org/10.1146/annurev-micro-020518-115555.
3. Orr MW, Donaldson GP, Severin GB, Wang J, Sintim HO, Waters CM, Lee VT. 2015. Oligoribonuclease is the primary degradative enzyme for pGpG in *Pseudomonas aeruginosa* that is required for cyclic-di-GMP turnover. Proc Natl Acad Sci U S A 112:E5048–E5057. https://doi.org/10.1073/pnas.1507245112.
4. Sondermann H, Shikuma NJ, Yildiz FH. 2012. You've come a long way: C-di-GMP signaling. Curr Opin Microbiol 15:140–146. https://doi.org/10.1016/j.mib.2011.12.008.
5. Wang YC, Chin KH, Le Tu Z, He J, Jones CJ, Sanchez DZ, Yildiz FH, Galperin MY, Chou SH. 2016. Nucleotide binding by the widespread high-affinity cyclic di-GMP receptor MshEN domain. Nat Commun 7:12481. https://doi.org/10.1038/ncomms12481.
6. Schäper S, Steinchen W, Krol E, Altegoer F, Skotnicka D, Søgaard-Andersen L, Bange G, Becker A. 2017. AraC-like transcriptional activator CuxR binds c-di-GMP by a PilZ-like mechanism to regulate extracellular polysaccharide production. Proc Natl Acad Sci U S A 114:E4822–E4831. https://doi.org/10.1073/pnas.1702435114.
7. Pérez-Mendoza D, Rodríguez-Carvajal MÁ, Romero-Jiménez L, Farias GDA, Lloret J, Gallegos MT, Sanjuán J. 2015. Novel mixed-linkage β -glucan activated by c-di-GMP in *Sinorhizobium meliloti*. Proc Natl Acad Sci U S A 112:E757–E765. https://doi.org/10.1073/pnas.1421748112.
8. Wang Y, Xu J, Chen A, Wang Y, Zhu J, Yu G, Xu L, Luo L. 2010. GGDEF and EAL proteins play different roles in the control of *Sinorhizobium meliloti* growth, motility, exopolysaccharide production, and competitive nodulation on host alfalfa. Acta Biochim Biophys Sin (Shanghai) 42:410–417. https://doi.org/10.1093/abbs/gmq034.
9. Pérez-Mendoza D, Aragón IM, Prada-Ramírez HA, Romero-Jiménez L, Ramos C, Gallegos M-T, Sanjuán J. 2014. Responses to elevated c-di-GMP levels in mutualistic and pathogenic plant-interacting bacteria. PLoS One 9:e91645. https://doi.org/10.1371/journal.pone.0091645.
10. Gao S, Ben Romdhane S, Beullens S, Kaever V, Lambrichts I, Fauvart M, Michiels J. 2014. Genomic analysis of cyclic-di-GMP-related genes in rhizobial type strains and functional analysis in *Rhizobium etli*. Appl Microbiol Biotechnol 98:4589–4602. https://doi.org/10.1007/s00253-014-5722-7.
11. Schäper S, Krol E, Skotnicka D, Kaever V, Hilker R, Søgaard-Andersen L, Becker A. 2016. Cyclic di-GMP regulates multiple cellular functions in the symbiotic alphaproteobacterium *Sinorhizobium meliloti*. J Bacteriol 198:521–535. https://doi.org/10.1128/JB.00795-15.
12. Schäper S, Wendt H, Bamberger J, Sieber V, Schmid J, Becker A. 2019. A bifunctional UDP-sugar 4-epimerase supports biosynthesis of multiple cell surface polysaccharides in *Sinorhizobium meliloti*. J Bacteriol 201:e00801-18. https://doi.org/10.1128/JB.00801-18.
13. Zipfel C, Oldroyd GED. 2017. Plant signalling in symbiosis and immunity. Nature 543:328–336. https://doi.org/10.1038/nature22009.
14. Udvardi M, Poole PS. 2013. Transport and metabolism in legume-rhizobia symbioses. Annu Rev Plant Biol 64:781–805. https://doi.org/10.1146/annurev-arplant-050312-120235.
15. Toft C, Andersson SGE. 2010. Evolutionary microbial genomics: insights into bacterial host adaptation. Nat Rev Genet 11:465–475. https://doi.org/10.1038/nrg2798.
16. Abel S, Bucher T, Nicollier M, Hug I, Kaever V, Abel Zur Wiesch P, Jenal U. 2013. Bi-modal distribution of the second messenger c-di-GMP controls cell fate and asymmetry during the *Caulobacter* cell cycle. PLoS Genet 9:e1003744-11. https://doi.org/10.1371/journal.pgen.1003744.
17. Solano C, García B, Latasa C, Toledo-Arana A, Zorraquino V, Valle J, Casals J, Pedroso E, Lasa I. 2009. Genetic reductionist approach for dissecting individual roles of GGDEF proteins within the c-di-GMP signaling network in *Salmonella*. Proc Natl Acad Sci U S A 106:7997–8002. https://doi.org/10.1073/pnas.0812573106.
18. Tian CF, Zhou YJ, Zhang YM, Li QQ, Zhang YZ, Li DF, Wang S, Wang J, Gilbert LB, Li YR, Chen WX. 2012. Comparative genomics of rhizobia nodulating soybean suggests extensive recruitment of lineage-specific genes in adaptations. Proc Natl Acad Sci U S A 109:8629–8634. https://doi.org/10.1073/pnas.1120436109.
19. Li YZ, Wang D, Feng XY, Jiao J, Chen WX, Tian CF. 2016. Genetic analysis reveals the essential role of nitrogen phosphotransferase system components in *Sinorhizobium fredii* CCBAU 45436 symbioses with soybean and pigeonpea plants. Appl Environ Microbiol 82:1305–1315. https://doi.org/10.1128/AEM.03454-15.
20. Liu LX, Li QQ, Zhang YZ, Hu Y, Jiao J, Guo HJ, Zhang XX, Zhang B, Chen WX, Tian CF. 2017. The nitrate-reduction gene cluster components exert lineage-dependent contributions to optimization of *Sinorhizobium* symbiosis with soybeans. Environ Microbiol 19:4926–4938. https://doi.org/10.1111/1462-2920.13948.
21. Jiao J, Tian C-F. 2020. Ancestral zinc-finger bearing protein MucR in alpha-proteobacteria: a novel xenogeneic silencer? Comput Struct Biotechnol J 18:3623–3631. https://doi.org/10.1016/j.csbj.2020.11.028.
22. Jiao J, Wu LJ, Zhang B, Hu Y, Li Y, Zhang XX, Guo HJ, Liu LX, Chen WX, Zhang Z, Tian CF. 2016. MucR is required for transcriptional activation of conserved ion transporters to support nitrogen fixation of *Sinorhizobium fredii* in soybean nodules. Mol Plant Microbe Interact 29:352–361. https://doi.org/10.1094/MPMI-01-16-0019-R.
23. Jiao J, Ni M, Zhang B, Zhang Z, Young JPW, Chan T-F, Chen WX, Lam H-M, Tian CF. 2018. Coordinated regulation of core and accessory genes in the multipartite genome of *Sinorhizobium fredii*. PLoS Genet 14:e1007428. https://doi.org/10.1371/journal.pgen.1007428.
24. Cui W, Zhang B, Zhao R, Liu L, Jiao J, Zhang Z, Tian C-F. 2021. Lineage-specific rewiring of core pathways predating innovation of legume nodules shapes symbiotic efficiency. mSystems 6:1–18. https://doi.org/10.1128/mSystems.01299-20.
25. Sarenko O, Klauck G, Wilke FM, Pfiffer V, Richter AM, Herbst S, Kaever V, Hengge R. 2017. More than enzymes that make or break cyclic di-GMP—local signaling in the interactome of GGDEF/EAL domain. mBio 8:1–18. https://doi.org/10.1128/mBio.01639-17.
26. Zähringer F, Massa C, Schirmer T. 2011. Efficient enzymatic production of the bacterial second messenger c-di-GMP by the diguanylate cyclase YdeH from *E. coli*. Appl Biochem Biotechnol 163:71–79. https://doi.org/10.1007/s12010-010-9017-x.
27. Poole P, Ramachandran V, Terpolilli J. 2018. Rhizobia: from saprophytes to endosymbionts. Nat Rev Microbiol 16:291–303. https://doi.org/10.1038/nrmicro.2017.171.
28. Henry JT, Crosson S. 2011. Ligand-binding PAS domains in a genomic, cellular, and structural context. Annu Rev Microbiol 65:261–286. https://doi.org/10.1146/annurev-micro-121809-151631.
29. Schmidt AJ, Ryjenkov DA, Gomelsky M. 2005. The ubiquitous protein domain EAL is a cyclic diguanylate-specific phosphodiesterase: enzymatically active and inactive EAL domains. J Bacteriol 187:4774–4781. https://doi.org/10.1128/JB.187.14.4774-4781.2005.
30. Tal R, Wong HC, Calhoon R, Gelfand D, Fear AL, Volman G, Mayer R, Ross P, Amikam D, Weinhouse H, Cohen A, Sapir S, Ohana P, Benziman M. 1998. Three cdg operons control cellular turnover of cyclic di-GMP in *Acetobacter xylinum*: genetic organization and occurrence of conserved domains in isoenzymes. J Bacteriol 180:4416–4425. https://doi.org/10.1128/JB.180.17.4416-4425.1998.

31. Seefeldt LC, Peters JW, Beratan DN, Bothner B, Minteer SD, Raugei S, Hoffman BM. 2018. Control of electron transfer in nitrogenase. Curr Opin Chem Biol 47:54–59. https://doi.org/10.1016/j.cbpa.2018.08.011.
32. Baena I, Pérez-Mendoza D, Sauviac L, Francesch K, Martín M, Rivilla R, Bonilla I, Bruand C, Sanjuán J, Lloret J. 2019. A partner-switching system controls activation of mixed-linkage β-glucan synthesis by c-di-GMP in *Sinorhizobium meliloti*. Environ Microbiol 21:3379–3391. https://doi.org/10.1111/1462-2920.14624.
33. Subramanian S, Kearns DB. 2019. Functional regulators of bacterial flagella. Annu Rev Microbiol 73:225–246. https://doi.org/10.1146/annurev-micro-020518-115725.
34. Li Y, Tian CF, Chen WF, Wang L, Sui XH, Chen WX. 2013. High-resolution transcriptomic analyses of *Sinorhizobium* sp. NGR234 bacteroids in determinate nodules of *Vigna unguiculata* and indeterminate nodules of *Leucaena leucocephala*. PLoS One 8:e70531. https://doi.org/10.1371/journal.pone.0070531.
35. Hu Y, Jiao J, Liu LX, Sun YW, Chen W, Sui X, Chen W, Tian CF. 2018. Evidence for phosphate starvation of rhizobia without terminal differentiation in legume nodules. Mol Plant Microbe Interact 31:1060–1068. https://doi.org/10.1094/MPMI-02-18-0031-R.
36. Zhang P, Zhang B, Jiao J, Dai S-Q, Chen W-X, Tian C-F. 2020. Modulation of symbiotic compatibility by rhizobial zinc starvation machinery. mBio 11:e03193-19. https://doi.org/10.1128/mBio.03193-19.
37. Crespo-Rivas JC, Navarro-Gómez P, Alias-Villegas C, Shi J, Zhen T, Niu Y, Cuéllar V, Moreno J, Cubo T, Vinardell JM, Ruiz-Sainz JE, Acosta-Jurado S, Soto MJ. 2019. *Sinorhizobium fredii* HH103 RirA is required for oxidative stress resistance and efficient symbiosis with soybean. Int J Mol Sci 20:787. https://doi.org/10.3390/ijms20030787.
38. Acosta-Jurado S, Alias-Villegas C, Navarro-Gomez P, Zehner S, Del Socorro Murdoch P, Rodríguez-Carvajal MA, Soto MJ, Ollero FJ, Ruiz-Sainz JE, Göttfert M, Vinardell JM. 2016. The *Sinorhizobium fredii* HH103 MucR1 global regulator is connected with the nod regulon and is required for efficient symbiosis with *Lotus burttii* and *Glycine max* cv. Williams. Mol Plant Microbe Interact 29:700–712. https://doi.org/10.1094/MPMI-06-16-0116-R.
39. Fumeaux C, Radhakrishnan SK, Ardissone S, Théraulaz L, Frandi A, Martins D, Nesper J, Abel S, Jenal U, Viollier PH. 2014. Cell cycle transition from S-phase to G1 in *Caulobacter* is mediated by ancestral virulence regulators. Nat Commun 5:4081. https://doi.org/10.1038/ncomms5081.
40. Baglivo I, Pirone L, Malgieri G, Fattorusso R, Roop RM, Pedone EM, Pedone PV. 2018. MucR binds multiple target sites in the promoter of its own gene and is a heat-stable protein: is MucR a H-NS-like protein? FEBS Open Bio 8:711–718. https://doi.org/10.1002/2211-5463.12411.
41. Pirone L, Pitzer JE, D'Abrosca G, Fattorusso R, Malgieri G, Pedone EM, Pedone PV, Roop RM, Baglivo I. 2018. Identifying the region responsible for *Brucella abortus* MucR higher-order oligomer formation and examining its role in gene regulation. Sci Rep 8:17238. https://doi.org/10.1038/s41598-018-35432-1.
42. Russo L, Palmieri M, Caso JV, Abrosca GD, Diana D, Malgieri G, Baglivo I, Isernia C, Pedone PV, Fattorusso R. 2015. Towards understanding the molecular recognition process in prokaryotic zinc-finger domain. Eur J Med Chem 91:100–108. https://doi.org/10.1016/j.ejmech.2014.09.040.
43. Malgieri G, Palmieri M, Russo L, Fattorusso R, Pedone PV, Isernia C. 2015. The prokaryotic zinc-finger: structure, function and comparison with the eukaryotic counterpart. FEBS J 282:4480–4496. https://doi.org/10.1111/febs.13503.
44. Close TJ, Tait RC, Kado CI. 1985. Regulation of Ti plasmid virulence genes by a chromosomal locus of *Agrobacterium tumefaciens*. J Bacteriol 164:774–781. https://doi.org/10.1128/jb.164.2.774-781.1985.
45. Zhan HJ, Levery SB, Lee CC, Leigh JA. 1989. A second exopolysaccharide of *Rhizobium meliloti* strain SU47 that can function in root nodule invasion. Proc Natl Acad Sci U S A 86:3055–3059. https://doi.org/10.1073/pnas.86.9.3055.
46. Keller M, Roxlau A, Weng WM, Schmidt M, Quandt J, Niehaus K, Jording D, Arnold W, Puhler A. 1995. Molecular analysis of the *Rhizobium meliloti mucR* gene regulating the biosynthesis of the exopolysaccharides succinoglycan and galactoglucan. Mol Plant Microbe Interact 8:267–277. https://doi.org/10.1094/mpmi-8-0267.
47. Chou AY, Archdeacon J, Kado CI. 1998. *Agrobacterium* transcriptional regulator Ros is a prokaryotic zinc finger protein that regulates the plant oncogene *ipt*. Proc Natl Acad Sci U S A 95:5293–5298. https://doi.org/10.1073/pnas.95.9.5293.
48. Mendis HC, Madzima TF, Queiroux C, Jones KM. 2016. Function of succinoglycan polysaccharide in *Sinorhizobium meliloti* host plant invasion depends on succinylation, not molecular weight. mBio 7:e00606-16. https://doi.org/10.1128/mBio.00606-16.
49. Cooley MB, D'Souza MR, Kado CI. 1991. The *virC* and *virD* operons of the *Agrobacterium* Ti plasmid are regulated by the *ros* chromosomal gene: analysis of the cloned ros gene. J Bacteriol 173:2608–2616. https://doi.org/10.1128/jb.173.8.2608-2616.1991.
50. Mueller K, Gonzalez JE. 2011. Complex regulation of symbiotic functions is coordinated by MucR and quorum sensing in *Sinorhizobium meliloti*. J Bacteriol 193:485–496. https://doi.org/10.1128/JB.01129-10.
51. Caswell CC, Elhassanny AEM, Planchin EE, Roux CM, Weeks-Gorospe JN, Ficht T. a, Dunman PM, Martin Roop R. 2013. Diverse genetic regulon of the virulence-associated transcriptional regulator MucR in *Brucella abortus* 2308. Infect Immun 81:1040–1051. https://doi.org/10.1128/IAI.01097-12.
52. Bittinger MA, Milner JL, Saville BJ, Handelsman J. 1997. *rosR*, a determinant of nodulation competitiveness in *Rhizobium etli*. Mol Plant Microbe Interact 10:180–186. https://doi.org/10.1094/MPMI.1997.10.2.180.
53. Baglivo I, Russo L, Esposito S, Malgieri G, Renda M, Salluzzo A, Di Blasio B, Isernia C, Fattorusso R, Pedone PV. 2009. The structural role of the zinc ion can be dispensable in prokaryotic zinc-finger domains. Proc Natl Acad Sci U S A 106:6933–6938. https://doi.org/10.1073/pnas.0810003106.
54. Bertram-Drogatz PA, Quester I, Becker A, Puhler A. 1998. The *Sinorhizobium meliloti* MucR protein, which is essential for the production of high-molecular-weight succinoglycan exopolysaccharide, binds to short DNA regions upstream of *exoH* and *exoY*. Mol Gen Genet 257:433–441. https://doi.org/10.1007/s004380050667.
55. Cheng HP, Walker GC. 1998. Succinoglycan is required for initiation and elongation of infection threads during nodulation of alfalfa by *Rhizobium meliloti*. J Bacteriol 180:5183–5191. https://doi.org/10.1128/JB.180.19.5183-5191.1998.
56. Bahlawane C, McIntosh M, Krol E, Becker A. 2008. *Sinorhizobium meliloti* regulator MucR couples exopolysaccharide synthesis and motility. Mol Plant Microbe Interact 21:1498–1509. https://doi.org/10.1094/MPMI-21-11-1498.
57. Jenal U, Reinders A, Lori C. 2017. Cyclic di-GMP: second messenger extraordinaire. Nat Rev Microbiol 15:271–284. https://doi.org/10.1038/nrmicro.2016.190.
58. Krol E, Schäper S, Becker A. 2020. Cyclic di-GMP signaling controlling the free-living lifestyle of alpha-proteobacterial rhizobia. Biol Chem 401:1335–1348. https://doi.org/10.1515/hsz-2020-0232.
59. Marx CJ, Lidstrom ME. 2002. Broad-host-range *cre-lox* system for antibiotic marker recycling in gram-negative bacteria. Biotechniques 33:1062–1067. https://doi.org/10.2144/02335rr01.
60. Quandt J, Hynes MF. 1993. Versatile suicide vectors which allow direct selection for gene replacement in Gram-negative bacteria. Gene 127:15–21. https://doi.org/10.1016/0378-1119(93)90611-6.
61. Sun Y-W, Li Y, Hu Y, Chen W-X, Tian C-F. 2019. Coordinated regulation of the size and number of polyhydroxybutyrate granules by core and accessory phasins in the facultative microsymbiont *Sinorhizobium fredii* NGR234. Appl Environ Microbiol 85:e00717-19. https://doi.org/10.1128/AEM.00717-19.
62. Zhu B, Liu C, Liu S, Cong H, Chen Y, Gu L, Ma LZ. 2016. Membrane association of SadC enhances its diguanylate cyclase activity to control exopolysaccharides synthesis and biofilm formation in *Pseudomonas aeruginosa*. Environ Microbiol 18:3440–3452. https://doi.org/10.1111/1462-2920.13263.
63. Bähre H, Kaever V. 2017. Identification and quantification of cyclic di-guanosine monophosphate and its linear metabolites by reversed-phase LC-MS/MS. Methods Mol Biol 1657:45–58. https://doi.org/10.1007/978-1-4939-7240-1_5.
64. Langmead B, Salzberg SL. 2012. Fast gapped-read alignment with Bowtie 2. Nat Methods 9:357–359. https://doi.org/10.1038/nmeth.1923.
65. Anders S, Pyl PT, Huber W. 2015. HTSeq A Python framework to work with high-throughput sequencing data. Bioinformatics 31:166–169. https://doi.org/10.1093/bioinformatics/btu638.